Interplay between structure and dynamics in adaptive complex networks: Emergence and amplification of modularity by adaptive dynamics

Wu-Jie Yuan[1,2] and Changsong Zhou[1,*]

[1]*Department of Physics, Hong Kong Baptist University, Kowloon Tong, Hong Kong, China*

[2]*College of Physics and Electronic Information, Huaibei Normal University, Huaibei 235000, China*

(Received 1 December 2010; revised manuscript received 27 May 2011; published 29 July 2011)

Many real networks display modular organization, which can influence dynamical clustering on the networks. Therefore, there have been proposals put forth recently to detect network communities by using dynamical clustering. In this paper, we study how the feedback from dynamical clusters can shape the network connection weights with a weight-adaptation scheme motivated from Hebbian learning in neural systems. We show that such a scheme generically leads to the formation of community structure in globally coupled chaotic oscillators. The number of communities in the adaptive network depends on coupling strength c and adaptation strength r. In a modular network, the adaptation scheme will enhance the intramodule connection weights and weaken the intermodule connection strengths, generating effectively separated dynamical clusters that coincide with the communities of the network. In this sense, the modularity of the network is amplified by the adaptation. Thus, for a network with a strong community structure, the adaptation scheme can evidently reflect its community structure by the resulting amplified weighted network. For a network with a weak community structure, the statistical properties of synchronization clusters from different realizations can be used to amplify the modularity of the communities so that they can be detected reliably by the other traditional algorithms.

DOI: 10.1103/PhysRevE.84.016116 PACS number(s): 89.75.Fb, 05.45.Xt, 87.18.Sn

I. INTRODUCTION

Many real-world systems from nature to society can be described by complex networks [1,2]. These networks often exhibit topological characteristics that are far from random, such as small-world and scale-free properties. Also, many networks display modular structure, in which network nodes are linked together in tightly knit communities, or modules, between which there are only looser connections [3]. This property has been observed in many systems, including social and biological networks [3,4]. Such a community structure can play concrete functional roles. For example, in a food web, communities reveal the subsystems of an ecosystem [5]. Thus, it is important to study community structure for complex dynamical systems.

Most of the previous studies on community networks have been focused on developing methods to identify community structure [3–12]. In particular, there have been several proposals to use synchronization and dynamical clustering to detect communities [14–17]. This is based on the understanding that structure plays a fundamental role in shaping various dynamics of complex systems [18–20]. In addition to detection of a community using synchronization, the impact of community on dynamics has received a great deal of attention. For example, it was found that [21] the dynamics exhibits a hierarchical modular organization in complex cortical brain networks. In a gradient clustered network, in which the sizes of the clusters are distributed unevenly, the synchronizability of the network is determined mainly by the properties of the subnetworks in the two largest clusters if the gradient field is sufficiently strong [22]. For a multimodular network (allowing nodes to simultaneously belong to two or more communities), the dynamical behavior is enhanced in each interface of the graph modules, so the overlapping structure can be identified by a careful monitoring of the synchronization process [23].

Recently, there have also been a few attempts to study how and why communities emerge in complex networks [24,25]. For example, it has been shown that (unweighted) modular configurations emerge from multiconstraint optimization, e.g., minimizing the average path length and the total number of links while maximizing robustness against perturbations in node activity [24]. Community topology can appear by adding links, where the weights are generated dynamically according to a local search of the developing topology [25].

However, the investigations on topological models for the emergence of community and the impact of community on dynamical clusters do not take into consideration an important ingredient in many realistic network systems. Many real-world networks are interacting dynamical entities with an interplay between dynamical states and network topology, which are so-called adaptive networks (AN's) [26,27]. In the past few years, models of AN's have been presented and investigated [26,28–31]. For instance, Ref. [26] has investigated adaptive changes of coupling strength due to a local synchronization property in heterogeneous networks. Reference [28] has proposed a traffic-driven adaptive model of weighted technological networks, where the traffic and topology mutually interact. Reference [29] has studied consensus formation by considering adaptive rewiring of links according to a similarity of views. Here, it is natural to expect that the adaptive mechanism has an influence on the formation of community structure.

Large-scale social networks are known to satisfy the "weak links" hypothesis [32] with the implication that links within communities are strong whereas links between them are weak [25]. That is to say, when taking the weights into consideration, the modularity of the network will be larger. In this paper, we propose a simple but generic adaptive model in which the

*cszhou@hkbu.edu.hk

scheme of weight adaptation motivated from Hebbian learning in neural systems can lead to a weighted community structure during the course of the adaptive evolution. The strengths of connection are enhanced if the links are within the community and are weakened if the links are between the communities, and gradually the network is broken into synchronization clusters. In this way, the modularity is amplified by the adaptation scheme so that the resulting weighted network can evidently exhibit the community structure of the original network. Therefore, there exists a potential application of the adaptive scheme: in networks with weak communities, this adaptation scheme can first amplify modularity and then efficiently detect the weighted communities by combining the statistical properties of the synchronization clusters with the established methods, such as the Potts [10], signal [11], weighted extremal optimal (WEO) [12], weighted Girvan-Newman (WGN) [7] algorithms, and so on. In this paper, we adopt the traditional and more precise [11] WGN method.

The paper is organized as follows. We introduce the adaptive model in Sec. II. In Sec. III, we show that the model generically generates modular structure in globally coupled chaotic oscillators. In Sec. IV, we show that the model can be used to amplify modularity efficiently for the detection of communities.

II. ADAPTIVE MODEL

We consider N coupled identical chaotic oscillators

$$\dot{\mathbf{x}}_i = \mathbf{F}(\mathbf{x}_i) + \frac{c}{K}\sum_{j=1}^{N} A_{ij} W_{ij}[\mathbf{H}(\mathbf{x}_j) - \mathbf{H}(\mathbf{x}_i)], \qquad (1)$$

where $\mathbf{F}(\mathbf{x})$ is the dynamics of individual oscillators, $\mathbf{H}(\mathbf{x})$ is a coupling function, and c is the coupling strength, which is normalized by the average degree K of the network. A_{ij} is the adjacency matrix ($A_{ij} = 1$ or 0) and $W_{ij} (i \neq j)$ is the weight of the connection from node j to node i ($W_{ij} \geqslant 0$).

In the adaptive network, the weight is not static, but evolves with time due to the feedback from the synchronization dynamics. We adopt an adaptation scheme motivated from Hebbian learning in neural systems: the coupling strength between two nodes is strengthened if synchronization occurs between them [30,33]. Also, we consider that the growth of the weight is limited because the coupling strength cannot increase indefinitely [30,34]. With the above consideration, the weight dynamics is given by

$$\dot{W}_{ij} = -W_{ij} + e^{-r\Delta_{ij}}, \qquad (2)$$

where $\Delta_{ij} = |\mathbf{x}_i - \mathbf{x}_j|$ is the state distance between nodes i and j, and $r > 0$ is an adaptation parameter. When r is large, the weight evolution is sensitive to the synchronization properties. When r approaches zero, the connection weights will be uniform in the network and will take an asymptotic value $W_{ij} = 1$.

We can expect that such a scheme will lead to the formation of heterogeneous connection strengths: when two nodes synchronize better, the connection will be strengthened to improve the synchronization further, while two nodes with weak synchronization may be effectively decoupled due to reduced coupling weight and become even more independent in dynamics. In community networks, such a scheme is expected to make the communities more pronounced, therefore it could amplify the modularity.

III. EMERGENCE OF COMMUNITY STRUCTURE IN A GLOBALLY COUPLED NETWORK OF CHAOTIC OSCILLATORS

To gain insight into the emergence of modularity, we consider a globally coupled chaotic Rössler oscillator: $\mathbf{x} = (x,y,z)$ and $\mathbf{F}(\mathbf{x}) = [-0.97y - z, 0.97x + 0.15y, z(x - 8.5) + 0.4]$. In addition, $\mathbf{H}(\mathbf{x}) = \mathbf{x} = (x,y,z)$ is adopted. The main results, however, do not depend on the particular properties of the chaotic oscillator and coupling function.

In the following, we present the results of our numerical simulations of the adaptive network. In the simulations, we use the fourth Runge-Kutta method to integrate Eqs. (1) and (2) with time step 0.01. The number of nodes N is set to 100, though the results described below are qualitatively similar for larger systems except for a longer computing time. The system starts with initial values randomly chosen from the chaotic attractor, and initial weight $W_{ij} = 0.1$ for all links.

The formation of community structure in the adaptive network can be quantified by modularity. A weighted modularity Q_m^W for the possible number of communities, m, is introduced in [7],

$$Q_m^W = \frac{1}{2S}\sum_{ij}\left(W_{ij} - \frac{s_i s_j}{2S}\right)\delta(m_i, m_j), \qquad (3)$$

where the δ function $\delta(u,v)$ is 1 if $u = v$ and 0 otherwise, $s_i = \sum_j W_{ij}$ is the total weight of node i, $S = \frac{1}{2}\sum_{ij} W_{ij}$ is the sum of all the connecting weights in the graph, and m_i is the community to which node i is assigned. The modularity is a property of a network and a specific proposed division of that network into communities [7]. Its high values correspond to good divisions of the weighted network into communities. Therefore, we can calculate the number of communities M of the best division by maximizing the modularity Q_m^W as Q^W. In this section, we adopt the WGN algorithm [7] to find communities of the adaptive network.

From the results of our simulations, we find that community structure can emerge during the time evolution to achieve complete synchronization eventually. Figure 1(a) displays the maximal modularity Q^W and the corresponding number M of communities as a function of evolutionary time. Here, we apply the WGN method to the resulting weighted network at every time interval 50. It is seen that a modular structure appears quickly and changes immediately to another modular structure. This indicates that the evolution at the beginning is a fast transient process, which is mainly due to the transient formation of small effective synchronization clusters [see Fig. 1(b)] due to initial conditions. Later on, such small clusters merge to form larger clusters, which can persist for quite a long time. Here, we focus on such a persistent community structure. The snapshots in Figs. 1(c) and 1(d) show that the network is split into groups with strong couplings within groups and weaker couplings between groups, effectively forming communities.

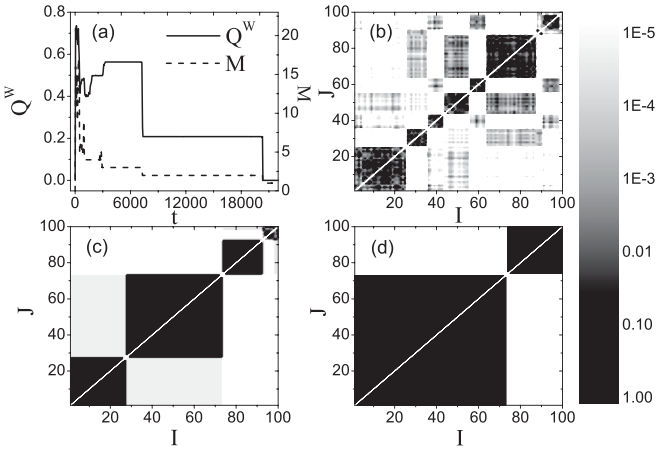

FIG. 1. Evolution of the maximal weighted modularity Q^W and the corresponding number of communities M as a function of time t in the globally coupled adaptive network (a) and gray-scale plots of the resulting weights W_{ij} at different time $t = 250$ (b), $t = 2000$ (c), and $t = 10\,000$ (d). Here the node index is resorted as I and J according to communities. The parameters are $c = 1.0$ and $r = 1.2$.

In our adaptive model, there are two important parameters: the coupling strength c, which determines the overall strength of the interactions between the nodes, and the adaptation parameter r, which controls the adaptive dynamics of weights and reflects adaptation strength. Now we investigate the dependence of the number of communities M on the two parameters c and r at a given time $t = 500$.

As shown in Fig. 2, the number of communities M decreases as coupling strength c becomes larger for a given r, because the oscillators achieve larger-scale synchronization at stronger couplings. This result is consistent with the effect of the coupling strength on the formation of an ordered phase in globally coupled maps [30]. As c increases to a large enough value, the community structure will disappear ($M = 1$). In Fig. 2, we show that for a given c, the community structure emerges ($M > 1$) when r is larger than a threshold value. The network will form a larger number of communities when r increases further, because now the connection weight is very sensitive to different synchronization levels according to the adaptive scheme in Eq. (2).

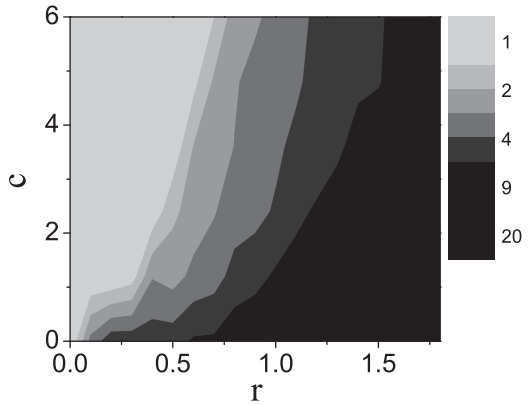

FIG. 2. Phase diagram of the number of communities M in the r-c plane. Data are averaged over 20 independent runs.

IV. COMMUNITY AMPLIFICATION BY ADAPTIVELY DYNAMICAL CLUSTERING

Motivated by the above observations of the emergence of community structure from the adaptive model, we expect that the adaptation scheme can amplify the modularity in community networks. In the adaptive process, the connecting weights within a community could be increased, but the connecting weights among communities reduced. Consequently, as the weights W_{ij} adaptively evolve, the module structure can be amplified by the resulting weighted network and the network dynamical state can emerge into clusters of synchronized elements (i.e., "cluster synchronization" state) in accordance with the underlying community structure present in the network. The adaptation scheme in Eq. (2) shows that there are two fixed points of weight values:

$$W_{ij} = \begin{cases} 1 & (\Delta_{ij} = 0), \\ 0 & (\Delta_{ij} \gg 0). \end{cases} \tag{4}$$

During the course of achieving cluster synchronization, the intracluster weights will approach 1 while intercluster weights will approach 0. However, the fixed point $W_{ij} = 0$ is unstable, and the network can eventually achieve a complete synchronization state. Therefore, we can judge whether the system has achieved the state of effective synchronization clusters by monitoring the following quantity:

$$\sigma = \frac{1}{\sum_{ij} W_{ij}} \sum_{ij} W_{ij} \Delta_{ij}, \tag{5}$$

which will take a small value, because either W_{ij} or Δ_{ij} will be quite small for such a state. In our simulations, the cluster synchronization is considered to be achieved when σ reaches 10^{-7}.

To study the amplification of modularity, we consider a random unweighted community network model [35]: N nodes are classified into M groups, each group having $n = N/M$ nodes. Within any group, each pair of nodes is connected with probability p_s, and between groups, the nodes are connected with probability p_l. In this paper, we take $N = 200$, $M = 4$, and $p_s = 0.6$, respectively. Clearly, the network with $p_l < p_s$ has four communities. As p_l increases from small values, the resulting community structure becomes progressively weaker and the networks pose greater challenges to the community-detecting algorithms. The networks are simulated with the chaotic Rössler oscillators. We start with the same initial weights $W_{ij}(0)$ for all the connections. Throughout this section, $W_{ij}(0)$ is set to 0.1 in an unweighted network, but the results described below are quite similar for other values of $W_{ij}(0)$ in the region (0,1). The nonconnecting weights are always kept at 0 during the course of evolution. So, a corresponding initial weighted network structure is given by the matrix W_0, which has the same community structure and modularity of the unweighted community network (matrix A). Starting from random initial conditions on the chaotic attractors, the weighted network evolves without adaptation at a weak-coupling strength $c_0 = 1.0$ for some time $t_r = 250$, so that the system can relax to weakly clustered synchronization states. Then the network begins the adaptive evolution according to Eq. (2) with a certain stronger value of c.

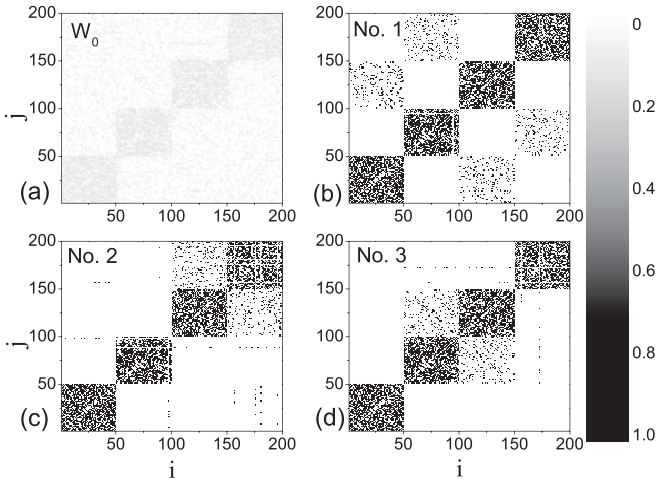

FIG. 3. The case of a strong community network with $p_l = 0.1$. The initial weight matrix W_0 (a) is compared to the resulting weight matrices (b), (c), and (d) of three realizations from random initial conditions. Here the parameters are $c = 11$ and $r = 8$.

For the strong community structure, we show in Fig. 3 that the resulting weighted network can well amplify the original community structure when cluster synchronization is achieved: the connection weights W_{ij} within the community are much stronger than those between communities. Indeed, the modularity Q_m^W of the resulting networks becomes much larger than that of original network W_0 by using the WGN method [Fig. 4(a)]. The best partition at maximal modularity of the resulting weighted network can recover the network communities correctly, as seen in Fig. 4(b) by the fraction of correctly identified nodes, $R \simeq 1$. In this paper, we use a quite harsh definition for the fraction R as in Ref. [6]: "We find the largest set of vertices that are grouped together in each of the known communities. If we put two or more of these sets in the same group, then all vertices in those sets are considered incorrectly classified. Otherwise, they are considered correctly classified. All other vertices not in the largest sets are considered incorrectly classified." Interestingly, for each given partition with m communities, we find that the modularity Q_m^W of the weighted network from adaptation is linearly related to the corresponding modularity Q_m^A of the underlying unweighted network [Fig. 4(c)], with an amplification ratio $\sim$1.5 for all the three realizations shown here. Here Q_m^A is obtained by applying Eq. (3) to the network adjacency matrix A for the corresponding partitions obtained from the weighted networks from adaptation.

For the network with strong enough communities, the amplification of modularity may not be necessary for the detection of the community, because the Girvan-Newman (GN) method can already identify the community correctly using the original matrix A. However, the situation becomes quite different for networks with weak communities. An example is shown in Figs. 5 and 6. In this case, the communities are so weak [Fig. 5(a)] that the WGN method cannot find any partition with significant modularity: Q_m^W for W_0 is very small for all partitions [Fig. 6(a)]. However, the adaptation process can lead to clearly clustered networks: the connection weights within the communities become clearly stronger

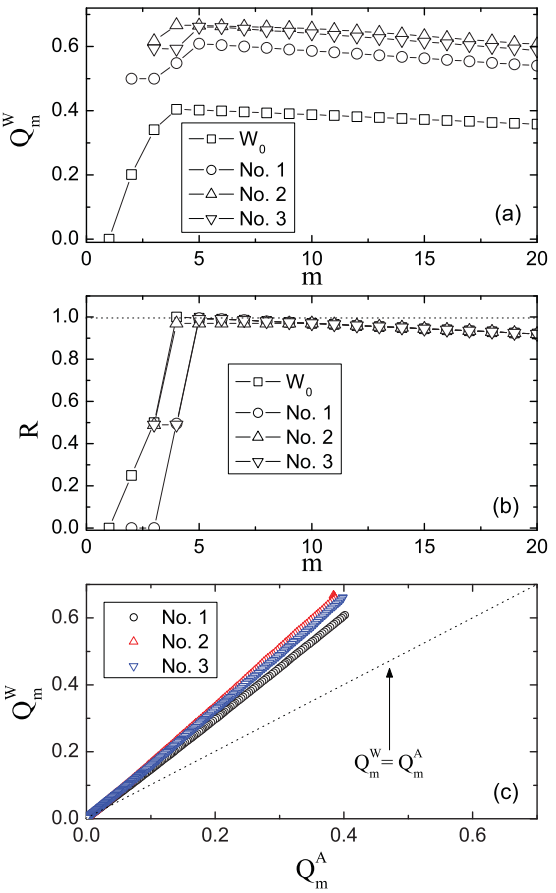

FIG. 4. (Color online) Amplification of modularity in a network with strong communities at $p_l = 0.1$. (a) The modularity Q_m^W of the resulting weight matrices in Figs. 3(a)–3(d) as a function of the possible number of communities m. (b) The fraction of R of nodes correctly classified into the underlying community. (c) The modularity Q_m^W of all the partitions from the resulting weighted network vs the corresponding modularity Q_m^A of the underlying unweighted network $A = (A_{ij})$ for the same partitions.

than those between the communities [Figs. 5(b)–5(d)]. Consequently, the modularity is significantly larger [Fig. 6(a)], and the communities reflected by the weighted networks from adaptive synchronization are consistent with the underlying topological partitions, as seen by the linear amplification of the modularity Q_m^W from the corresponding Q_m^A [Fig. 6(c)]. For some realizations [Figs. 5(b) and 5(d)], the communities can be reliably detected using the resulting weighted network, with the maximal $R \simeq 1$ [Fig. 6(b)]. But for some other realizations, two or more communities can appear to be in a big community in the resulting weighted networks [e.g., Fig. 5(c)], corresponding to lower Q_m^W and R in Figs. 6(a) and 6(b).

These results suggest a new way to improve the detection of weak communities by amplification of the modularity. Since the adaptive scheme depends on the parameters c and r, we can obtain realizations of weighted networks with various c, r, and random initial conditions. Applying the WGN method to each weighted network, we can get one partition of the network into communities. We can compute the modularity Q^A from the original matrix A for this partition. The partition is a better one

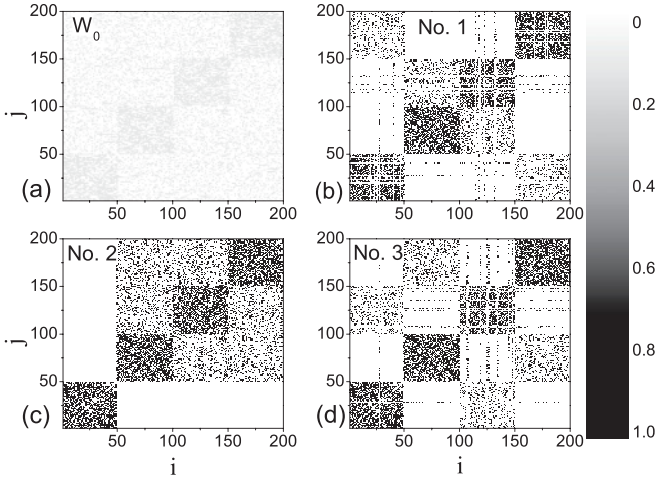

FIG. 5. The same as in Fig. 3, but for a weak community network with $p_l = 0.20$.

if Q^A is larger. For all the realizations, we can get a distribution of Q^A. Now we can select those "good" weighted networks with $Q^A > Q_{\rm th}$ and build a new matrix $P = (P_{ij})$ to measure the probability P_{ij} that nodes i and j are found to belong to a common community among these "good" realizations. Of course, $Q_{\rm th}$ cannot be larger than the maximal modularity Q_{p_l} for the known communities of the underlying network

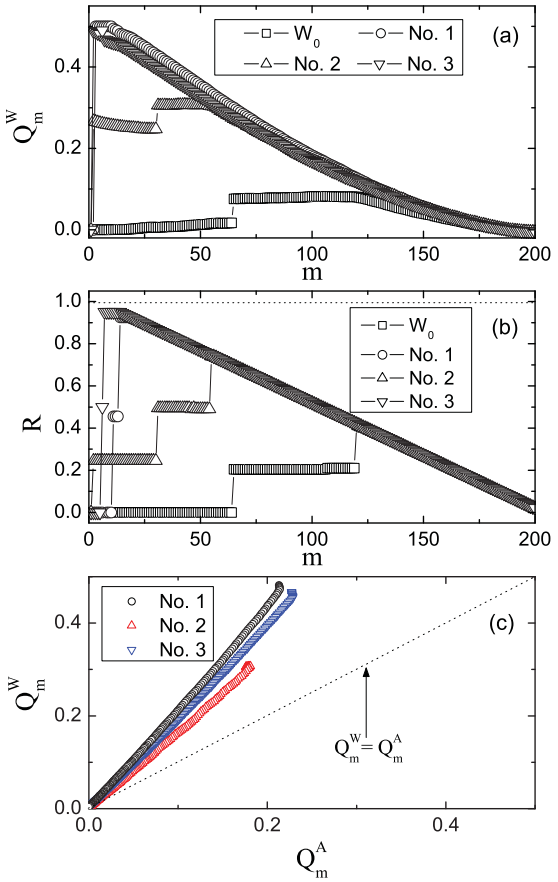

FIG. 6. (Color online) The same as in Fig. 4, but for a weak community network at $p_l = 0.20$ [as Fig. 5(a)].

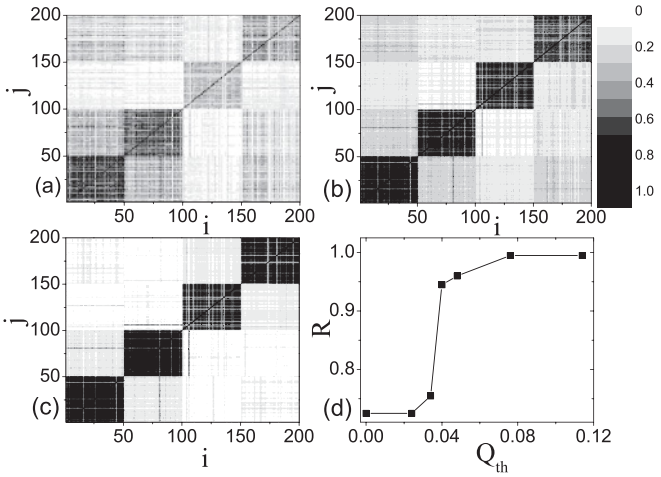

FIG. 7. Detection of weak community ($p_l = 0.25$) by amplifying the modularity using the matrix $P = (P_{ij})$ at various thresholds $Q_{\rm th} = 0.0$ (a), $Q_{\rm th} = 0.08$ (b), and $Q_{\rm th} = 0.11$ (c). (d) The fraction R of nodes classified correctly as a function of threshold $Q_{\rm th}$. Data of probability P_{ij} are measured over 50 independent runs with uniformly randomly chosen $4 < c < 10$, $8 < r < 58$, and initial conditions.

$A = (A_{ij})$. Examples of the matrices P at various threshold values $Q_{\rm th}$ are shown in Fig. 7 for community structure with $p_l = 0.25$, even weaker than that in Figs. 5 and 6. We can see that the weak community structure of the original network is significantly amplified in P, especially for large enough thresholds, because in these selected realizations, a pair of nodes from a common community in the underlying network will appear with high probability in the same community of the resulting weighted networks due to enhanced connection strength by adaptation. Now applying the WGN method to this amplified matrix P, we can detect the community reliably, as seen by the increasing R as a function of the threshold $Q_{\rm th}$. Note that R is already a good value $R > 0.7$ for $Q_{\rm th} = 0$ while the WGN method directly applied to the original network gives $R \approx 0.21$. For larger $Q_{\rm th}$, the cost we have to pay in this procedure is that we need to generate more realizations to allow enough realizations with $Q^A > Q_{\rm th}$.

A systematic examination of the performance of the amplification by our adaptation scheme is shown in Fig. 8, where we plot the fraction R of nodes correctly assigned to the four known communities as a function of p_l in the original community networks. For comparison, we also show the performance of the GN algorithm [7] directly applied to the original network matrix $A = (A_{ij})$. Our adaptive amplification scheme performs well, correctly identifying more and more fractions of nodes as the threshold $Q_{\rm th}$ increases. Therefore, for any given weak community network, its community structure can be identified to some extent by applying a certain traditional method to the resulting matrix P if we select a suitably large threshold for enough computing time.

To further test the performance of our amplification scheme, we have considered a large number of computer-generated random graphs with known community structure, as in Refs. [6,15]. Each graph consists of $N = 128$ nodes divided equally into four communities. Each node has on average $Z_{\rm in}$ links belonging to the same community and $Z_{\rm out}$ links

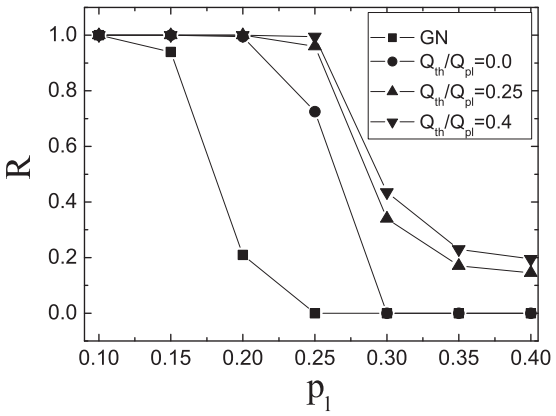

FIG. 8. The fraction R of nodes correctly identified by our adaptive amplification with different relative thresholds Q_{th}/Q_{p_l}, where Q_{p_l} is the corresponding modularity for the division of four known communities of the network with intercommunity connection probability p_l. R obtained by applying the GN algorithm to the original network $A = (A_{ij})$ is also given for a comparison. Data of probability P_{ij} are measured over 50 independent runs with uniformly randomly chosen $4 < c < 10$, $8 < r < 58$, and initial conditions.

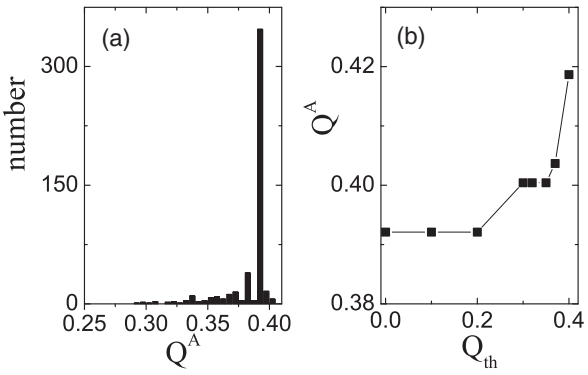

FIG. 10. (a) The histogram of the modularity Q^A for the partitions obtained from 500 weighted network realizations obtained from the adaptive process with uniformly randomly chosen $4 < c < 10$, $0 < r < 5$, and initial conditions in the "karate club" network of Zachary. (b) The modularity Q^A for the partitions obtained from P of various thresholds Q_{th} by using our adaptive scheme in the Zachary network. Data of probability P_{ij} are measured over 50 independent runs with uniformly randomly chosen $4 < c < 10$, $0 < r < 5$, and initial conditions.

belonging to different communities, where Z_{in} and Z_{out} are chosen so that the average degree $Z_{\text{in}} + Z_{\text{out}} = 16$. As Z_{out} increases, the resulting community structure becomes weaker and thus harder to detect. To comparatively evaluate the performance of our amplification scheme, we first show the results of several existing methods in Fig. 9(a), adapted from Ref. [15]. In Fig. 9(b), we report our results by using the amplification scheme. It is found that, as the threshold Q_{th} increases, the performance of our adaptation scheme can approach that of the best methods reported in Fig. 9(a), such as the OCR-HK [15] and simulated annealing (SA) [8] algorithms.

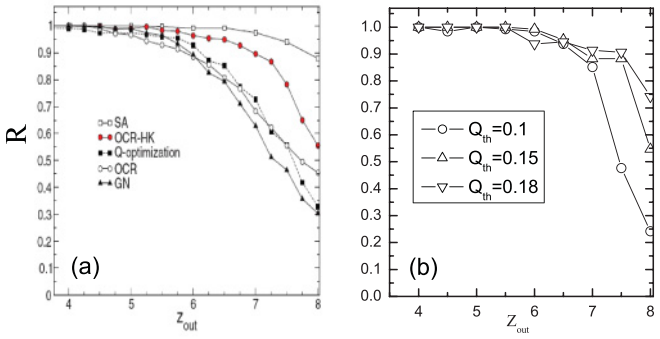

FIG. 9. (Color online) The fraction R of nodes correctly identified as a function of Z_{out} for computer-generated graphs described in Refs. [6,15] by using existing standard methods, such as GN [7], opinion changing rate (OCR) [15], the Newman Q optimization fast algorithm [6], opinion changing rate by Hegselmann-Krause (OCR-HK) [15], and the simulated annealing algorithm [8] (a) (adapted from Ref. [15]), and our adaptation scheme for different thresholds Q_{th} (b). Data of probability P_{ij} are measured over 50 independent runs with uniformly randomly chosen $4 < c < 10$, $8 < r < 58$, and initial conditions in (b).

Except for the above two types of computer-generated random networks with known communities, we have also applied our amplification scheme to a real-world network, namely the Zachary network [36]. We can obtain realizations of weighted networks by using the adaptation scheme with various c, r, and random initial conditions. Applying the WGN method to each weighted network, we get one partition of the network into communities. Then, we compute the modularity Q^A from the original matrix A for this partition. For all the realizations, we get a distribution of Q^A, as shown in Fig. 10(a). Obviously, most of the realizations have a modularity $Q^A \sim 0.39$, indicating that the resulting dynamical clusters by using our adaptation scheme can effectively reflect the community structure of the Zachary network. According to the distribution, we can choose a suitably large threshold to build the matrix $P = (P_{ij})$ for amplifying the modularity and then gain better partitions by using the WGN method for P. As shown in Fig. 10(b), we detect communities with higher modularity Q^A as the increase of threshold Q_{th}. Even in the absence of threshold (i.e., $Q_{\text{th}} = 0.0$), our adaptation scheme can also detect a better partition with modularity $Q^A = 0.3921$, which is larger than $Q^A = 0.3810$ obtained using the Newman Q-optimization method [6] and the signal method [11]. Furthermore, we gain $Q^A = 0.4187$ at $Q_{\text{th}} = 0.4$, which is approximately equal to the largest $Q^A = 0.4188$ obtained using the extremal optimal algorithm [12] among the reported results using other methods in the literature, such as Pujol-Béjar-Delgado (PBD) ($Q^A = 0.3937$) [13], OCR-HK ($Q^A \sim 0.40$) [15], and extremal optimal (EO) ($Q^A = 0.4176$) reported by Ref. [13]. This result strongly indicates that our adaptive amplification scheme works well in the real community network.

Finally, we have applied our adaptation scheme with the Hebbian learning rule to a real-world neural system, namely the cortical brain network of a cat [37], which is a weighted and directed network. This system possesses a small number of clusters that approximately agree with the four functional

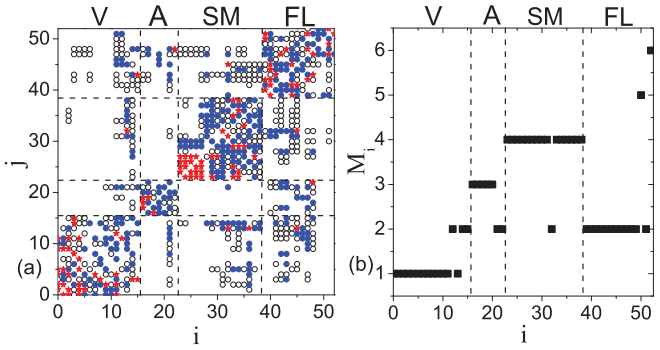

FIG. 11. (Color online) (a) The cortical network of a cat. A node represents a functional region of the cortex and a link represents the existence of fiber projection between two regions. The different symbols represent different connection weights: 1 (sparse: black ○), 2 (intermediate: blue •), and 3 (dense: red ∗). The network is organized into four topological communities [38] that broadly agree with the four functional cortical subdivisions, i.e., visual (V), auditory (A), somato-motor (SM), and fronto-limbic (FL). The functional subdivision of the networks is indicated by the dashed lines. (b) The partition into six communities by applying the WGN method directly to the matrix in (a).

cortical subdivisions, i.e., visual cortex (V), auditory (A), somato-motor (SM), and fronto-limbic (FL) [38], shown as Fig. 11(a) for the weighted coupling matrix W_0. The modularity of this functional subdivision is $Q^{W_0} = 0.363$. If we apply the WGN method directly to the matrix W_0, we can obtain a partition with modularity $Q^{W_0} = 0.342$, which is roughly consistent with the functional subdivision [Fig. 11(b)].

For the weighted network, all the weights were first normalized against the maximal weight before applying our scheme. The resulting normalized weighted network W_0 has the same community structure and modularity of the original weighted network. Then, we implemented the adaptive dynamics on the normalized weighted network W_0 with various c and r to obtain weighted network realizations, and we applied the WGN algorithm to these networks to obtain the community partition for each of the realizations. We can compute for these partitions the modularity Q^{W_0} based on the original network matrix W_0. The distribution of Q^{W_0} shown in Fig. 12(a) has a similar meaning to that in Fig. 10(a), and displays several peaks. The multimodal distribution reflects different groups of realizations where many nodes from a functional subsystem (e.g., V) can merge with many nodes from other subsystems to form various combinations of big communities, and it is related to heterogeneous communities in the brain network. We note that such a multimodal distribution does not exist in our previous network models with homogeneous communities (results not shown). Therefore, the distribution could be used to infer qualitatively the complexity of community structure, which will be addressed in future work. According to the distribution of Q^{W_0} in Fig. 12(a), we can choose a suitably large threshold $Q_{\rm th}$ to build the matrix $P = (P_{ij})$ and detect the community structure using the WGN method for P. As shown in Fig. 12(b), the modularity Q^P of the matrix P increases with $Q_{\rm th}$. Figure 12(c) shows that the modularity Q^{W_0} for the partitions obtained from the matrix P also increases with $Q_{\rm th}$. $Q^P > Q^{W_0}$ demonstrates again the amplification of

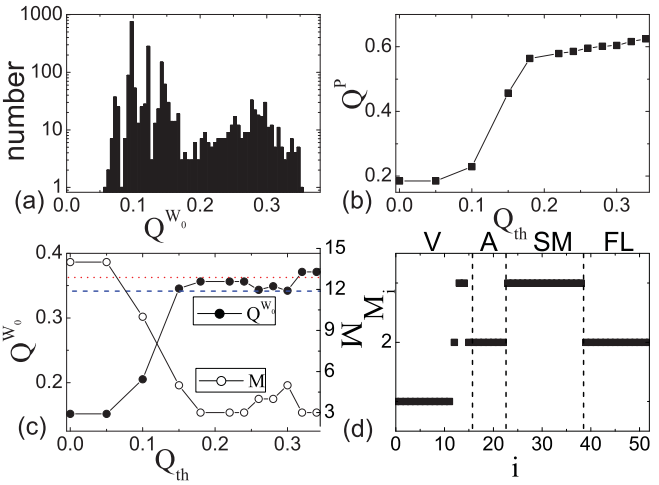

FIG. 12. (Color online) (a) The histogram of the modularity Q^{W_0} for the partitions obtained from 2000 weighted network realizations obtained from the adaptive process with uniformly randomly chosen $4 < c < 10$, $8 < r < 58$, and initial conditions. (b) The modularity Q^P of the matrix $P = (P_{ij})$, obtained by applying the WGN algorithm to P corresponding to various thresholds $Q_{\rm th}$. (c) The modularity Q^{W_0} and number of communities M for the partitions obtained from P of various thresholds $Q_{\rm th}$ by using our adaptation scheme in the cortical brain network of a cat. Red dot-dashed line: modularity $Q^{W_0} = 0.363$ of the functional subdivision in Fig. 11(a). Blue dashed line: modularity $Q^{W_0} = 0.342$ of the partition in Fig. 11(b) obtained directly by the WGN method on the cortical network of a cat. (d) The partition into three communities at $Q_{\rm th} > 0.3$. Data of probability P_{ij} are measured over 200 independent runs with uniformly randomly chosen $4 < c < 10$, $8 < r < 58$, and initial conditions.

modularity by the adaptation process. In a range of $Q_{\rm th}$, the partitions obtained using our method have a modularity Q^{W_0} larger than the one obtained by applying the WGN method directly [blue dashed line in Fig. 12(c), $Q^{W_0} = 0.342$], but slightly below the modularity of the functional subdivision in Fig. 11(a) [37] [red dot-dashed line in Fig. 12(c), $Q^{W_0} = 0.363$]. The number of communities ranges from three to five. Interestingly, with larger $Q_{\rm th}$, we find a partition with three communities [Fig. 12(d)] whose modularity $Q^{W_0} = 0.372$ is larger than the functional subdivision in Fig. 11(a).

These results show that the WGN method, when applied to the cat cortical network directly, may not find the partition with maximal modularity. This difficulty may result from a special hierarchical modular organization in this system. There are hub nodes that form a hypercommunity overlapping on the four functional subsystems V, A, SM, and FL, which is of special importance for information integration of the system [39]. These brain regions from the hypercommunity are involved into multimodal functional performance [21,40]. Our adaptive dynamics provides a way to explore many possible combinations of brain regions from functional subsystems into different communities. Such rich combinations could be of functional relevance during particular cognitive processes when particular subsystems [e.g., A and FL in Fig. 12(d)] are required to be integrated for certain advanced information processing. We will study this problem in more detail in the context of the capacity and complexity of this complex network to support various forms of functional performance [41].

V. CONCLUSION

We study the emergence and amplification of modularity in adaptive networks in which the connection strength is enhanced due to synchronization between the oscillators, motivated by the Hebbian learning rule in neural networks. If a pair of nodes synchronize better, the connection weight is likely increased to improve the synchronization further. On the other hand, for weakly synchronized pairs, the connection weight has higher probability to decay and this makes the oscillators effectively decoupled. In globally coupled networks, such initial fluctuations in synchronization can lead to the formation of effectively disconnected modules during the transition to complete synchronization. In community networks, the effective synchronization clusters become correlated with the underlying network community. More importantly, the resulting weighted network amplifies the modular structure of original network due to strong intramodule connections and weak intermodule connections. Therefore, by introducing statistical properties of synchronization clusters from different realizations of the network, the weak community structure can be identified to some extent, even if it is too weak to be detected efficiently by using the traditional algorithms. Moreover, our numerical experimental results indicate that 50 realizations satisfying the threshold condition can be enough to stably amplify community structure. For the networks with high heterogeneity (e.g., a network benchmark model [42], characterized by the high heterogeneity in the distributions of node degrees and community sizes), our adaptation scheme can also produce dynamical clusters reflecting effectively the underlying community structure (results not shown). However, if we introduce statistical properties for different realizations, the amplification of community structure cannot be realized well. This is because even with similar modularity, the community structures of the resulting realizations can be very different from each other due to high heterogeneity. In summary, our investigation not only sheds light on the interaction and coevolution of structure and dynamics in complex network systems, but also provides a scheme to improve the detection of weak modular organization by adaptively amplifying the modularity.

Our study has also demonstrated that the Hebbian-like learning scheme can generically generate synchronization clusters and modular networks, indicating that such a dynamical scheme from the plasticity of synapses plays an important role in generating and maintaining the pronounced modular organization in neural systems [43]. In particular, the adaptive scheme may provide a useful tip for the understanding of the mechanism of spontaneous neuronal activity in the form of synchronized bursting events with several subgroups in developing cultured neuronal networks [44], which is an unaddressed fundamental issue regarding cellular mechanisms.

ACKNOWLEDGMENTS

This work is supported by Hong Kong Baptist University, the Hong Kong Research Grant Council No. HKBU202710, the National Natural Science Foundation of China under Grant No. 11005047, and the Young University Teacher's Fund of Anhui Province in China under Grant No. 2008jql071.

[1] R. Albert and A.-L. Barabási, Rev. Mod. Phys. **74**, 47 (2002).
[2] L. A. N. Amaral, A. Scala, M. Barthélemy, and H. E. Stanley, Proc. Natl. Acad. Sci. (USA) **97**, 11149 (2000).
[3] M. Girvan and M. E. J. Newman, Proc. Natl. Acad. Sci. (USA) **99**, 7821 (2002).
[4] M. E. J. Newman, Proc. Natl. Acad. Sci. (USA) **103**, 8577 (2006).
[5] R. J. Williams and N. D. Martinez, Nature (London) **404**, 180 (2000).
[6] M. E. J. Newman, Phys. Rev. E **69**, 066133 (2004).
[7] M. E. J. Newman, Phys. Rev. E **70**, 056131 (2004); M. Girvan and M. E. J. Newman, Proc. Natl. Acad. Sci. (USA) **99**, 7821 (2002); M. E. J. Newman and M. Girvan, Phys. Rev. E **69**, 026113 (2004).
[8] L. Danon, A. Díaz-Guilera, J. Duch, and A. Arenas, J. Stat. Mech.: Theory Exp. (2005) P09008; R. Guimerà, M. Sales-Pardo, and L. A. N. Amaral, Phys. Rev. E **70**, 025101(R) (2004).
[9] J. Reichardt and M. Leone, Phys. Rev. Lett. **101**, 078701 (2008).
[10] J. Reichardt and S. Bornholdt, Phys. Rev. Lett. **93**, 218701 (2004).
[11] Y. Hu, M. Li, P. Zhang, Y. Fan, and Z. Di, Phys. Rev. E **78**, 016115 (2008).
[12] J. Duch and A. Arenas, Phys. Rev. E **72**, 027104 (2005).
[13] J. M. Pujol, J. Béjar, and J. Delgado, Phys. Rev. E **74**, 016107 (2006).
[14] A. Arenas, A. Diaz-Guilera, and C. J. Perez-Vicente, Phys. Rev. Lett. **96**, 114102 (2006).
[15] S. Boccaletti, M. Ivanchenko, V. Latora, A. Pluchino, and A. Rapisarda, Phys. Rev. E **75**, 045102(R) (2007).
[16] E. Oh, C. Choi, B. Kahng, and D. Kim, Europhys. Lett. **83**, 68003 (2008).
[17] D. Gfeller and P. De Los Rios, Phys. Rev. Lett. **100**, 174104 (2008).
[18] J. Zhang, C. Zhou, X. Xu, and M. Small, Phys. Rev. E **82**, 026116 (2010).
[19] J. Ren, W.-X. Wang, B. Li, and Y.-C. Lai, Phys. Rev. Lett. **104**, 058701 (2010).
[20] T. C. Jarrett, D. J. Ashton, M. Fricker, and N. F. Johnson, Phys. Rev. E **74**, 026116 (2006).
[21] C. Zhou, L. Zemanová, G. Zamora, C. C. Hilgetag, and J. Kurths, Phys. Rev. Lett. **97**, 238103 (2006).
[22] X. Wang, L. Huang, Y.-C. Lai, and C. H. Lai, Phys. Rev. E **76**, 056113 (2007).
[23] J. A. Almendral, I. Leyva, D. Li, I. Sendiña-Nadal, S. Havlin, and S. Boccaletti, Phys. Rev. E **82**, 016115 (2010).
[24] R. K. Pan and S. Sinha, Phys. Rev. E **76**, 045103(R) (2007).
[25] J. M. Kumpula, J.-P. Onnela, J. Saramäki, K. Kaski, and J. Kertész, Phys. Rev. Lett. **99**, 228701 (2007).
[26] C. Zhou and J. Kurths, Phys. Rev. Lett. **96**, 164102 (2006).
[27] T. Gross and B. Blasius, J. R. Soc. Interface **5**, 259 (2008).
[28] W.-X. Wang, B.-H. Wang, B. Hu, G. Yan, and Q. Ou, Phys. Rev. Lett. **94**, 188702 (2005).

[29] B. Kozma and A. Barrat, Phys. Rev. E **77**, 016102 (2008).
[30] J. Ito and K. Kaneko, Phys. Rev. Lett. **88**, 028701 (2002); Phys. Rev. E **67**, 046226 (2003).
[31] Q. Ren and J. Zhao, Phys. Rev. E **76**, 016207 (2007).
[32] M. Granovetter, Am. J. Sociol. **78**, 1360 (1973).
[33] D. O. Hebb, *The Organization of Behavior* (Wiley, New York, 1949).
[34] T. Aoki and T. Aoyagi, Phys. Rev. Lett. **102**, 034101 (2009).
[35] L. Huang, K. Park, Y.-C. Lai, L. Yang, and K. Yang, Phys. Rev. Lett. **97**, 164101 (2006).
[36] W. W. Zachary, J. Anthropol. Res. **33**, 452 (1977).
[37] J. W. Scannell, G. A. P. C. Burns, C. C. Hilgetag, M. A. O'Neil, and M. P. Young, Cereb. Cortex **9**, 277 (1999).
[38] C. C. Hilgetag and M. Kaiser, Neuroinformatics **2**, 353 (2004).
[39] G. Zamora-López, C. Zhou, and J. Kurths, Chaos **19**, 015117 (2009); Front. Neuroinform. **4**, 1 (2010).
[40] L. Zemanová, C. Zhou, and J. Kurths, Physica D **224**, 202 (2006).
[41] M. Zhao, C. Zhou, Y. Chen, B. Hu, and B.-H. Wang, Phys. Rev. E **82**, 046225 (2010).
[42] A. Lancichinetti, S. Fortunato, and F. Radicchi, Phys. Rev. E **78**, 046110 (2008).
[43] D. Meunier, R. Lambiotte, and E. T. Bullmore, Front. Neurosci. **4**, 200 (2010).
[44] E. Hulata, I. Baruchi, R. Segev, Y. Shapira, and E. Ben-Jacob, Phys. Rev. Lett. **92**, 198105 (2004).